Resonance Raman Spectra and Vibrational Modes of Iron(III) Tetraphenylporphine μ-Oxo Dimer. Evidence for Phenyl Interaction and Lack of Dimer Splitting

J. M. Burke, J. R. Kincaid, and T. G. Spiro *

Contribution from the Department of Chemistry, Princeton University, Princeton, New Jersey 08540. Received March 13, 1978

Abstract: Resonance Raman spectra have been obtained for [Fe(TPP)]$_2$O (TPP = tetraphenylporphine) over a wide range of visible laser wavelengths. The bands are assigned to porphyrin vibrational modes on the basis of polarizations and deuterium shifts. Several resonance-enhanced phenyl modes are identified. A 5-cm^{-1} shift on ^{54}Fe substitution identifies a 363-cm^{-1} band with the symmetric Fe–O–Fe stretching mode. A previous claim of dimer vibrational splitting of porphyrin modes is not substantiated, and such splitting is shown to be too small in Fe(TPP)$_2$O to be detected. Excitation profiles are similar to those reported recently for CrTPPCl. Unusual aspects include 0–2 as well as 0–0 and 0–1 maxima for polarized modes at 1359 and 1553 cm^{-1}, and also "helping mode" behavior for the 390- and 363-cm^{-1} polarized bands, which maximize at the 0–1 position of the 1359-cm^{-1} band. In addition, a depolarized band at 1495 cm^{-1} shows 0–0, 0–1, and 0–2 maxima, suggestive of Jahn–Teller activity. The large origin shift implied for this mode, and for the 1359- and 1553-cm^{-1} polarized modes, as well as the observed resonance enhancement of phenyl modes, is consistent with a model of the excited state in which there is significant electron delocalization in the phenyl system, the steric strain of the required phenyl–methine bridge coplanarity being relieved by deformation of the porphyrin ring. Phenyl interaction in the ground state, however, is not required to explain any of the resonance Raman data.

Introduction

The structural chemistry of metalloporphyrins continues to be an active and productive research area. These molecules yield intense and detailed resonance Raman (RR) spectra which provide avenues both to theoretical elucidation of vibronic scattering mechanisms[1] and to structural applications.[2] While physiological porphyrins all have hydrogen atoms at the methine bridges and alkyl, vinyl, or formyl substituents on the pyrrole rings, much porphyrin chemistry has been explored with the tetraphenylporphines (TPP), which have methine phenyl substituents and hydrogen atoms on the pyrrole carbon atoms (see Figure 1). This alteration in the substitution pattern substantially modifies the composition of the porphyrin vibrational modes and also the scattering mechanisms. The latter have been the subject of several studies, but although numerous RR spectra of TPP derivatives have been reported,[1a,b,3] they have not been applied to structural questions, nor have the vibrations been analyzed.

In this study, we qualitatively assign the RR bands of the μ-oxo dimer of ferric TPP, [(TPP)Fe]$_2$O, with the aid of deuterium and ^{54}Fe isotope shifts. This derivative was chosen because its Q_0 and Q_v absorption bands lie in the dye laser tuning range of rhodamine 6G and sodium fluorescein, permitting detailed examination of the excitation wavelength dependence, leading to an unusually complete set of vibrational frequencies. Excitation profiles have been monitored and novel features relating to excited-state vibrational coupling have been observed.

Another aspect of the μ-oxo dimer which has attracted much interest[3b,4] is the relatively strong antiferromagnetic coupling between the bridged ferric ions. There is a possibility of antiferromagnetic heme–heme coupling in cytochrome oxidase,[5] and there is strong evidence that photosynthetic reaction centers contain a strongly coupled pair of chlorophyll molecules[6] (albeit with a quite different proposed geometry from that of the μ-oxo dimer). Adar and Srivastava[3b] have worked out the rules of vibrational coupling between two monomer units under conditions of RR scattering, and have offered evidence for vibrational splitting in [(TPP)Fe]$_2$O. Their candidate splittings can be ruled out, however, with the present, more complete data. We conclude that the coupling between the two

(TPP)Fe units is too weak to produce detectable vibrational shifts.

Experimental Section

Tetraphenylporphine (TPP) (Aldrich Chemical Co.) was purified by treatment with 2,3-dichloro-5,6-dicyanobenzoquinone (DDQ) followed by column chromatography on alumina (Fisher A-540).[7] TPP-d_8 was synthesized according to the method of Fajer et al.[8a] The resultant product was subsequently freed of chlorin.[7] TPP-d_{20} was synthesized from pyrrole and benzaldehyde-d_5 (EM Laboratories, Inc.) according to the method of Adler et al.[8b]

Incorporation of iron into the various TPP derivatives was carried out in dimethylformamide (DMF).[8c] The ^{54}Fe$_2$O$_3$, 75 mg (96.81% in ^{54}Fe, Oak Ridge National Laboratories), was placed within a quartz boat inside a quartz heating tube wrapped with Nichrome wire and insulated with asbestos and converted to the metal under a slow stream of H$_2$ at ~400 °C for 4 h, care being taken to eliminate all traces of O$_2$. The metal was transferred to a small Airless Ware flask, ~10 mL of methanol (freshly distilled and degassed) was added, and HCl gas was bubbled slowly to convert the sample to ^{54}FeCl$_2$. The HCl/methanol solution was evaporated to dryness and the white FeCl$_2$ was redissolved in ~10 mL of methanol. During these manipulations, care was taken to eliminate contact of materials with air, in order to avoid oxidation of the reduced iron. A portion of this methanol solution was added with a gas-tight syringe to a solution of TPP in DMF which had been refluxing under an argon atmosphere for ~20 min. Smaller portions were added until reaction was complete as indicated by lack of fluorescence under a long-wavelength ultraviolet light source (Black-Ray). Formation of [Fe(TPP)]$_2$O was accomplished by slow elution of FeTPPCl on Fisher A-540 alumina with chloroform.

Spectra were recorded on samples dissolved in methylene chloride (Burdick and Jackson Laboratories), carbon disulfide, tetrahydrofuran, or benzene, using the rotating cell technique. Argon ion (Spectra Physics 170, Coherent Radiation CR-5) and tunable dye (Spectra Physics 375 with rhodamine 6G, Coherent Radiation Model 490 with sodium fluorescein) lasers were used for excitation. The spectrometer has been described previously.[9]

Results and Discussion

A. Vibrational Analysis. 1. Symmetry Classification. Figure 2 shows RR spectra of [Fe(TPP)]$_2$O, while Table I gives a complete listing of the observed frequencies, divided into symmetry blocks according to the Raman polarizations: $\rho <$

Table I. Resonance Raman Bands (cm⁻¹) Observed for FeTPP Derivatives

	(FeTPP)₂O	(FeTPP-d₈)₂O	(FeTPP-d₂₀)₂O	FeTPPCl	[FeTPP(Im)₂]Cl	assignment[a]
			A_{1g} Block			
(A)	1599 (p)[b]	1599	1567	1605	1605 sh	phenyl
(1)	1553 (0.09)	1532	1553	1555	1568	$\nu(C_\beta-C_\beta) + \delta(C_\beta-H)$
(2)	1450 (0.09)	1428	1450	1454	1456	$\nu(C_\alpha-C_\beta) + \delta(C_\beta-H)$
(3)	1359 (0.06)	1348	1356	1366	1370	$\nu(C_\alpha-N) + \delta(C_\beta-H)$
(4)	1237 (0.08)	1234	1187	1240	1238	$\nu(C_m-Ph)$
(5)	1083 (p)	991	1083	1084	1084	$\delta(C_\beta-H)$
(B)	1030 (p)	1030	864		1029	phenyl
(6)	1004 (0.06)	1005	995	1009	1009	$\nu(C_\alpha-C_m)$
(C)	995 (p)	991	812			phenyl
(D)	886 (p)	886		890	890	phenyl
(7)	640 (p)	640	617	640	643	porphyrin deformation
(8)	390 (p)	382	390	390	390	porphyrin deformation
	363 (0.07)	363	363			$\nu(Fe-O)$
				334 (vw)	336 (vw)	
			A_{2g} Block			
(9)	1511 (13.7)	1511		1510	1540	$\nu(C_\alpha-C_m)$
(10)	1333 (10.9)	1263		1338	1340	$\nu(C_\alpha-C_\beta) + \delta(C_\beta-H)$
(11)	1234 (4.3)	1167		1225		$\nu(C_\alpha-N) + \delta(C_\beta-H)$
(12)	n.o.[c]					$\delta(C_\beta-H)$
(13)	827 (ap) vw					
(14)	n.o.					
(15)	n.o.					
			B_{1g} and B_{2g} Block			
(16)	1561 (dp)	1561	1561		1582	$\nu(C_\alpha-C_m)$ (B_{1g})
(17)	1495 (0.8)	1444	1496		1505	$\nu(C_\beta-C_\beta)$ (B_{1g})
(18)	1271 (dp)	1263		1270	1275	$\nu(C_\alpha-N)$
(19)	1087 (0.52)	995	1086	1084	1084	$\delta(C_\beta-H)$ (B_{1g})
(20)	1014 (0.68)	877	1014			$\delta(C_\beta-H)$ (B_{2g})
(21)	848 (0.87)	851				
(22)	257 (0.75)	257	257	256	232	
(23)	195 (dp)	195	195	202	204	

[a] See text for discussion of assignments. [b] p, polarized; ap, anomalously polarized; dp, depolarized. Where the depolarization could be measured with reasonable accuracy, the values are given in parentheses. [c] n.o.—expected, but not observed.
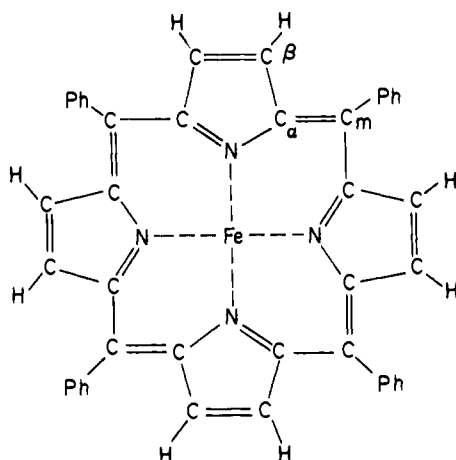
Figure 1. Structure of iron tetraphenylporphine (Ph = phenyl).

0.75 for A_{1g}, > 0.75 for A_{2g}, and 0.75 for B_{1g} and B_{2g} modes.

If the molecule has fourfold symmetry, then the A_{2g} modes should show infinite depolarization (inverse polarization).[10] Significant parallel components are often seen in anomalously polarized bands of metalloporphyrins, however, and are attributable either to symmetry lowering or to accidental degeneracy with polarized or depolarized modes.[11] A clear example of accidental degeneracy is the 1237-cm⁻¹ band of [Fe(TPP)]₂O, which exhibits depolarization ratios of 0.08 and 4.3 with 457.9- and 578.2-nm excitation, respectively, reflecting a superposition of A_{1g} and A_{2g} modes with different

excitation dependencies. This interpretation is confirmed by the different deuterium shifts of the two modes. The 827-cm⁻¹ ap mode is too weak for an accurate measurement of ρ. The values for the 1511- and 1333-cm⁻¹ band reflect a small parallel scattering component, about 10%. Whether this is significantly different from zero is difficult to tell, because of the background from nearby modes at 1495 and 1359 cm⁻¹.

B_{1g} and B_{2g} modes cannot be distinguished on the basis of depolarization ratios. There are never as many depolarized porphyrin bands observed as expected,[9] and examination of symmetry lowering correlations have suggested that B_{2g} modes are rarely active.[10,12]

For a planar scatter, ρ is expected to be $\frac{1}{8}$ for totally symmetric modes, corresponding to $\alpha_{xx} = \alpha_{yy}$ and $\alpha_{zz} = 0$, for the diagonal polarizability tensor elements. For the monomeric complexes included in this study, Fe(TPP)Cl and Fe(TPP)-$(Im)_2^+$, the polarized modes do indeed have $\rho = \frac{1}{8}$, within experimental error, although overlapping bands often render the determination inaccurate. This ratio also holds for the [Fe(TPP)]₂O polarized bands observed in the region of Q-band excitation, but it decreases significantly at shorter wavelengths. With 457.9-nm excitation, the recorded values ranged from 0.06 to 0.09 for the bands at 1237, 1359, 1450, and 1553 cm⁻¹. This lowering implies a nonnegligible contribution from α_{zz}. Resonance enhancement of this polarizability element depends upon z-polarized (out of plane) electronic transitions. We infer that [Fe(TPP)]₂O has high-energy out of plane transitions, presumably $O^{2-} \rightarrow Fe^{3+}$ charge transfer in character (vide infra), which exert a significant influence on the RR depolarization ratios at 457.9 nm. In the monomer complexes, such transitions are apparently weaker or located at higher energy.
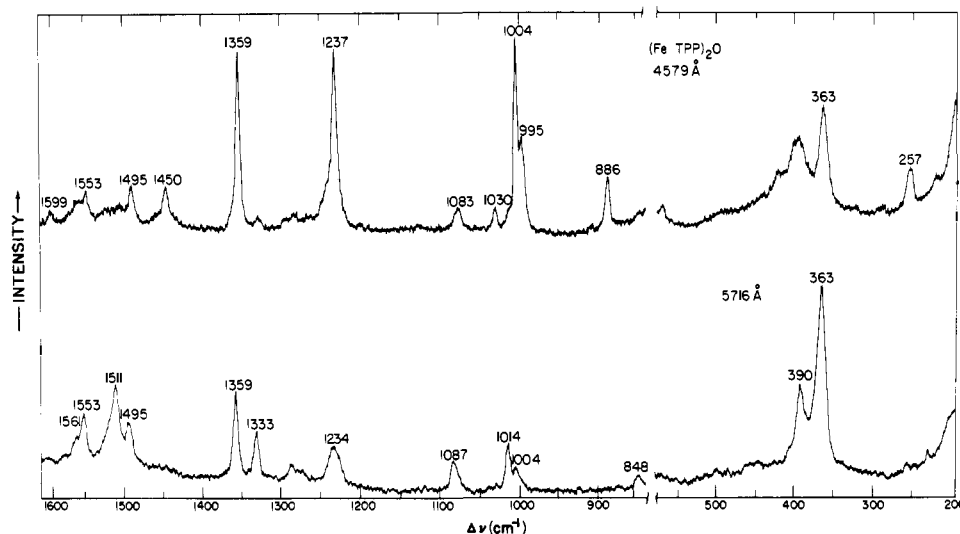
Figure 2. Resonance Raman spectra of [Fe(TPP)]$_2$O in CS$_2$, concentration 1 mg/mL.

2. Phenyl Modes. The RR spectrum contains more polarized bands than can be accounted for by the porphyrin skeleton. Examination of the frequency shifts on phenyl deuteration establishes that three bands, labeled A–C in Table I, arise from modes that are internal to the phenyl rings. They correspond in frequency and deuterium shift to well-characterized bands of monosubstituted benzenes.[13-15] An additional band, D, at 886 cm^{-1}, disappears upon phenyl deuteration. Its assignment is uncertain, since monosubstituted benzenes do not exhibit polarized bands in the 800–1000-cm^{-1} region.[13-15] Bands A–D are relatively weak, but they are definitely resonance enhanced; we estimate the enhancement relative to chlorobenzene in CS$_2$ to be roughly 10^3. Fuchsman et al.[16a] recently assigned a halogen-sensitive RR band of tetra(*p*-halophenyl)porphine derivatives in the region 1050–1100 cm^{-1} to a resonance-enhanced phenyl mode. This band is in addition to the 1083-cm^{-1} TPP porphyrin band[16b] (vide infra).

3. Porphyrin Modes. Since the absorption spectrum is dominated by porphyrin π–π* transitions, we expect, as usual, that the main RR bands correspond to in-plane porphyrin vibrations. Counting the phenyl rings as point masses, there are 53 such vibrations per Fe(TPP) monomer unit, assuming D_{4h} symmetry:

$$\Gamma_{\text{in-plane}} = 9A_{1g} + 8A_{2g} + 9B_{1g} + 9B_{2g} + 18E_u$$

The E$_u$ vibrations are infrared active only. One vibration in each of the remaining symmetry classes is a C–H stretching mode, expected at about 3000 cm^{-1}, and not observed in porphyrin RR spectra.

The main RR bands are found between 1000 and 1600 cm^{-1}, a region associated with C–C and C–N stretching and C–H deformation modes. Table II gives the expected contributions to each symmetry block of these internal coordinates, listed roughly in the order of the expected vibrational frequencies, based on the relative bond orders from structural data[17] (C$_\beta$-C$_\beta$ > C$_\alpha$-C$_m$ > C$_\alpha$-N > C$_\alpha$-C$_\beta$), and the expected frequencies for δ(C$_\beta$-H) modes. The atom labeling is defined in the structural diagram (Figure 1). The situation is quite different from the β-pyrrole substituted porphyrins[9] because the main kinematic interaction at the methine bridges is with ν(C$_m$-Ph), instead of δ(C$_m$-H), while the main interaction at the β-carbon atoms is with δ(C$_\beta$-H) instead of ν(C$_\beta$-C$_s$) (s = substituent). Also, δ(C$_m$-H) does not contribute to the A$_{1g}$ block of the pyrrole substituted hemes, because of symmetry, while δ(C$_\beta$-H) does contribute to the A$_{1g}$ block of TPP.

Table II predicts six A$_{1g}$ modes in the 1000–1600-cm^{-1} region, which are identified as bands 1–6 in Table I. Although

Table II. Symmetry Classification of TPP In-Plane C–C and C–N Stretching and C–H Bending Coordinates

A$_{1g}$	A$_{2g}$	B$_{1g}$	B$_{2g}$	E$_u$
C$_\beta$-C$_\beta$		C$_\beta$-C$_\beta$		C$_\beta$-C$_\beta$
C$_\alpha$-C$_m$	C$_\alpha$-C$_m$	C$_\alpha$-C$_m$	C$_\alpha$-C$_m$	C$_\alpha$-C$_m$
C$_\alpha$-N	C$_\alpha$-N	C$_\alpha$-N	C$_\alpha$-N	C$_\alpha$-N
C$_\alpha$-C$_\beta$	C$_\alpha$-C$_\beta$	C$_\alpha$-C$_\beta$	C$_\alpha$-C$_\beta$	C$_\alpha$-C$_\beta$
δC$_\beta$-H	δC$_\beta$-H	δC$_\beta$-H	δC$_\beta$-H	δC$_\beta$-H
C$_m$-C$_{Ph}$			C$_m$-C$_{Ph}$	C$_m$-C$_{Ph}$

the internal coordinates are undoubtedly highly mixed in the porphyrin normal modes, the deuterium shifts give an indication of the major contributors. Band 1 shifts appreciably on d_8 (β-carbon substitution) as expected for a large ν(C$_\beta$-C$_\beta$) contribution, and is the highest frequency nonphenyl A$_{1g}$ mode, consistent with the presumed double-bond character of the C$_\beta$-C$_\beta$ bond. Band 3, which gives one of the most intense polarized modes, is assigned to ν(C$_\alpha$-N) primarily by analogy to the intense band at ~1360 cm^{-1} in β-pyrrole substituted porphyrins, which the ^{15}N shift[18] shows to be a C$_\alpha$-N breathing mode. Band 4 is clearly assignable to ν(C$_m$-Ph) via its large (50 cm^{-1}) d_{20} (meso carbon) shift. This mode is analogous to the inter-ring stretch of biphenyl,[15] at 1277 cm^{-1}, which shifts about twice as far (89 cm^{-1}) on perdeuteration, as expected. The large d_8 shift (92 cm^{-1}) for band 5 requires that it have a major contribution from δ(C$_\beta$-H). This leaves band 2 (1450 cm^{-1}) and band 6 (1004 cm^{-1}) to be assigned to ν(C$_\alpha$-C$_m$) and ν(C$_\alpha$-C$_\beta$). The higher bond order of the C$_\alpha$-C$_m$ bond would suggest its assignment to the higher frequency, but this would be inconsistent with lack of any d_{20} shift, in view of the expected coupling with ν(C$_m$-Ph), and with the substantial d_8 shift, despite the lack of expected coupling with δ(C$_\beta$-H). This deuterium shift pattern is consistent instead with what is expected for ν(C$_\alpha$-C$_\beta$). Band 6 on the other hand shows no d_8 shift but a modest d_{20} shift, as expected for ν(C$_\alpha$-C$_m$). The reversal of the expected frequencies for these coordinates can be explained by kinematic coupling effects. ν(C$_\alpha$-C$_m$) may be strongly depressed by coupling with ν(C$_m$-Ph) while ν(C$_\alpha$-C$_\beta$) may be raised by coupling with δ(C$_\beta$-H). The coupling pattern would be reversed in β-pyrrole substituted porphyrins, for which the carbon substituents are on C$_\beta$ and the hydrogen atoms are attached to C$_m$.

Below 1000 cm^{-1}, two more A$_{1g}$ modes are expected, associated with ring deformation and Fe–N stretching. Bands 7 and 8 are assigned to these modes. β-Pyrrole substituted porphyrins also show A$_{1g}$ modes in the vicinity of 670 and 350
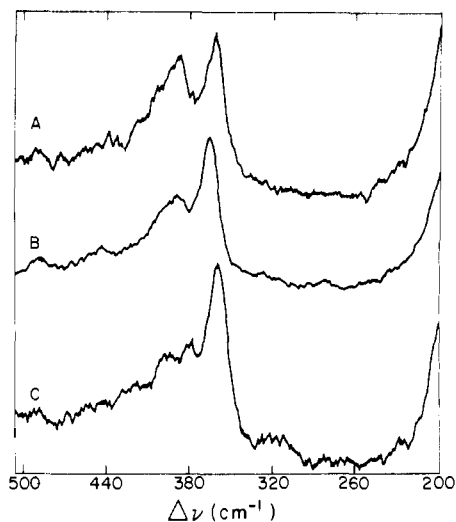
Figure 3. Low-frequency resonance Raman spectra in benzene (1 mg/mL) with 528.7-nm excitation: (A) [Fe(TPP)]$_2$O; (B) [^{54}Fe(TPP)]$_2$O; (C) [Fe(TPP)-d_8)]$_2$O.

cm^{-1}.[12] It is of interest that band 7 shows a d_{20} shift while band 8 shows a d_8 shift. Evidently the higher frequency mode involves movement of the methine bridge, while the lower frequency mode involves movement of the pyrrole rings.

In the A$_{2g}$ block, four modes are expected above 1000 cm^{-1}. Three are observed, at 1511, 1333, and 1234 cm^{-1}. The highest of these, band 9, shows no d_8 shift, and is assigned to $\nu(C_\alpha-C_m)$. The large frequency reduction due to $\nu(C_m-Ph)$ coupling, which is observed for this coordinate in the A$_{1g}$ block, is not seen in the A$_{2g}$ block, since there is no A$_{2g}$ C$_m$-Ph contribution. Band 10, at 1333 cm^{-1}, shifts 70 cm^{-1} on d_8 substitution, and is assigned to $\nu(C_\alpha-C_\beta)$. Band 11, at 1234 cm^{-1}, is then assigned to $\nu(C_\alpha-N)$. Its d_8 shift, 67 cm^{-1}, is larger than the 11-cm^{-1} shift observed for the A$_{1g}$ $\nu(C_\alpha-N)$ at 1359 cm^{-1}, and presumably reflects greater coupling with the A$_{2g}$ $\delta(C_\beta-H)$ mode, which is itself apparently too weak to be observed. Three more A$_{2g}$ modes are expected below 1000 cm^{-1}; one of these is observed at 827 cm^{-1}.

Eight depolarized bands are observed, although a total of 16 B$_{1g}$ and B$_{2g}$ modes are expected. B$_{2g}$ modes, however, are rarely seen in porphyrin RR spectra.[10,12] However, the 1014-cm^{-1} band (band 20), which shifts 137 cm^{-1} on d_8 substitution, is assignable to the B$_{2g}$ $\delta(C_\beta-H)$ mode, since the B$_{1g}$ $\delta(C_\beta-H)$ mode has the same phasing as the A$_{1g}$ $\delta(C_\beta-H)$ mode, band 5, at 1083 cm^{-1}, and is reasonably assigned to band 19 at 1087 cm^{-1}. Bands 5 and 19 show the same d_8 shifts, 92 cm^{-1}. Four other B$_{1g}$ modes are expected above 1000 cm^{-1}, and the three depolarized bands (16–18) at 1561, 1495, and 1271 cm^{-1} are assigned to these. Band 16 shows no d_8 shift and is assigned to $\nu(C_\alpha-C_m)$; as in the A$_{2g}$ block, there is no C$_m$-Ph mode with which to couple. Band 17 shows a large d_8 shift, 51 cm^{-1}, and is assigned to $\nu(C_\beta-C_\beta)$, while band 18 gives a small d_8 shift, and is assigned to $\nu(C_\alpha-N)$. A mode arising primarily from $\nu(C_\alpha-C_\beta)$ is apparently not observed. The three depolarized bands below 1000 cm^{-1} can be assigned to the remaining three expected B$_{1g}$ modes.

4. Fe–O–Fe Stretch. Substitution of ^{54}Fe shifts the 363-cm^{-1} polarized band up by 5 cm^{-1} (see Figure 3). No other shift is observed. In particular the 390-cm^{-1} band is unshifted; its deuterium shift is 8 cm^{-1} while there is no deuterium shift for the 363-cm^{-1} band. The latter is clearly assignable to the out of plane symmetric Fe–O–Fe stretch, while the 390-cm^{-1} band is an in-plane deformation mode (see above). To the extent that it contains a contribution from Fe–N stretching, it should be slightly iron-isotope sensitive, since the iron atom lies out of

the plane by 0.50 Å.[19a] The tilt of the Fe–N bonds with respect to the plane is sufficiently slight, however, that the ^{54}Fe/^{56}Fe isotope shift is not expected to be detectable.

The 363-cm^{-1} band is the symmetric counterpart of the asymmetric Fe–O–Fe stretch previously located in the infrared spectrum[19b] as a doublet at 892 and 878 cm^{-1} (average value 885 cm^{-1}). Using a model with an Fe–O–Fe angle of 175°[19b] these frequencies are calculated with an Fe–O stretching force constant of 3.8 mdyn/Å and a stretch–stretch interaction constant of 0.16 mdyn/Å if the effective iron mass is taken to be 56. These force constants are similar to those found for other oxo-bridged transition metal complexes.[20]

B. Intradimer Coupling. The foregoing analysis was based on the monomer Fe(TPP) vibrations, except for $\nu_{Fe-O-Fe}$. The dimer has two vibrational modes for each of the monomer modes, a symmetric and an antisymmetric combination. Only the symmetric set is Raman active if the dimer has a center of symmetry, but both sets can be active if the symmetry center is lost—e.g., by bending at the central oxygen atom or by a nonsymmetric relative disposition of the porphyrin rings. Even if both sets are active, however, they will remain degenerate unless the interaction strength is significant on the scale of vibrational energies.

Table I lists vibrational frequencies for Fe(TPP)Cl and Fe(TPP)(Im)$_2^+$, as well as [Fe(TPP)]$_2$O. Fe(TPP)Cl contains high-spin Fe(III), as does [Fe(TPP)]$_2$O, while Fe(TPP)(Im)$_2^+$ contains low-spin Fe(III). To the extent that dimer interactions are insignificant, the Fe(TPP)Cl frequencies are expected to lie close to those of [Fe(TPP)]$_2$O. This is indeed observed. All the A$_{1g}$ frequencies of [Fe(TPP)]$_2$O find close correspondences with those of Fe(TPP)Cl, with the exception of the 363-cm^{-1} Fe–O–Fe stretch, and the very weak 1030-cm^{-1} band, assigned to a phenyl mode, which is seen in Fe(TPP)(Im)$_2^+$. Close correspondences are also seen in the A$_{2g}$ and B$_{1g}$-B$_{2g}$ blocks, but several frequencies are missing for the monomeric complexes, particularly for Fe(TPP)Cl. The reason for this is simply that depolarized and anomalously polarized bands are less strongly enhanced for these species. The weakness of these bands may be connected[1b] to the lower Q$_0$ absorption intensity observed for the monomeric species. Since all the A$_{1g}$ and B$_{1g}$-B$_{2g}$ modes are reasonably assigned to monomer porphyrin vibrations, we find no evidence for dimer splitting.

Adar and Srivastava[3b] have previously analyzed the problem and have argued that [Fe(TPP)]$_2$O does in fact show dimer splitting in its RR spectra, suggesting a substantial interaction as well as symmetry lowering. Three instances of splitting were advanced on the basis of a comparison of Fe(TPP)Cl with [Fe(TPP)]$_2$O: 370 → 390 and 363, 1555 → 1553 and 1495, and 1518 → 1507 and 1512 cm^{-1}. As demonstrated by the ^{54}Fe shift, the 363-cm^{-1} band is the Fe–O–Fe stretch and not a component of the 390-cm^{-1} band. The 1553- and 1495-cm^{-1} bands are of different symmetry, and both have counterparts in the Fe(TPP)(Im)$_2^+$ spectrum. Finally, our spectra show only a single band at 1511 cm^{-1}, which can be readily distinguished from the nearby bands by its anomalous polarization. Although the band is broad, we cannot confirm a splitting.

A more sensitive measure of dimer interaction would be the appearance of infrared-active modes in the Raman spectrum and vice versa. For every monomer infrared mode, the out of phase dimer combination should be Raman active, while for every monomer Raman mode, the out of phase dimer combination should be infrared active. The extent of the dimer-induced activity, however, is difficult to predict. We have searched the infrared spectrum of [Fe(TPP)]$_2$O for coincidences with the observed porphyrin Raman modes. Many of the possible frequencies are obscured by interfering phenyl modes. However, we do observe a weak IR band at 1358 cm^{-1}, coincident with the strong A$_{1g}$ Raman mode, as shown in Figure 4. This band is absent in the IR spectrum of monomeric
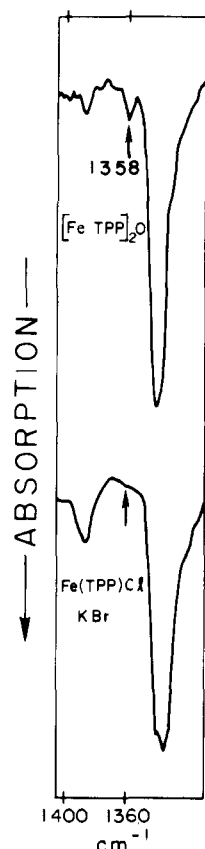
Figure 4. Infrared spectra of [Fe(TPP)]$_2$O (top) and Fe(TPP)Cl (bottom) obtained as KBr pellets (~2 mg per 250 mg KBr).

Figure 5. Resonance Raman excitation profiles of [Fe(TPP)]$_2$O. The visible absorption spectrum is shown at bottom of figure. Raman intensity is corrected for self-absorption.

Fe(TPP)Cl. The nearby strong band at 1344 cm^{-1}, seen in both spectra, is no doubt the corresponding E$_u$ mode. The weak 1358-cm^{-1} band is plausibly assigned to the out of phase combination of the monomer A$_{1g}$ modes. Its frequency is the same as that of the in-phase combination, seen in the Raman spectrum, suggesting that the dimer interaction does not produce a detectable splitting of the monomer modes. This is consistent with the relatively large separation (5.2 Å)[19a] of the porphyrin rings in the µ-oxo dimer, and the consequent absence of any direct orbital overlap between them. Any interaction must be transmitted through the intervening N–Fe and Fe–O bonds.

C. Excitation Profiles. Figure 5 shows excitation profiles for several Raman bands of [Fe(TPP)]$_2$O. They were obtained using the rhodamine 6G (566–616 nm) and sodium fluorescein (533–572 nm) dye laser tuning ranges, as well as the discrete Ar$^+$ laser lines. The data have been corrected for self-absorption.[21] Also shown is the absorption spectrum. The pair of absorption bands, 612 and 572 nm, are assignable as the 0–0 and 0–1 components of the porphyrin Q (α, β) band, while the rising portion below 540 nm is the beginning of the B (Soret) band which peaks at 408 nm. For the most part, the profiles are similar to those observed for CrTPPCl by Shelnutt et al.,[1b] who interpreted their features in terms of strong vibronic coupling between the Q and B states, superimposed on a small amount of Jahn–Teller activity in the Q state.

The A$_{2g}$ mode profiles all show a double-peaked profile in the Q band region. The separation between the profile maxima is, however, significantly less than the ground-state vibrational frequency of the mode being monitored. The apparent reduction is mainly due to the constructive interference expected for a vibronic (B term) mechanism, between 0–0 and 0–1 antisymmetric scattering components, which tends to draw the peaks together and fill in the valley.[22] This effect is accentuated
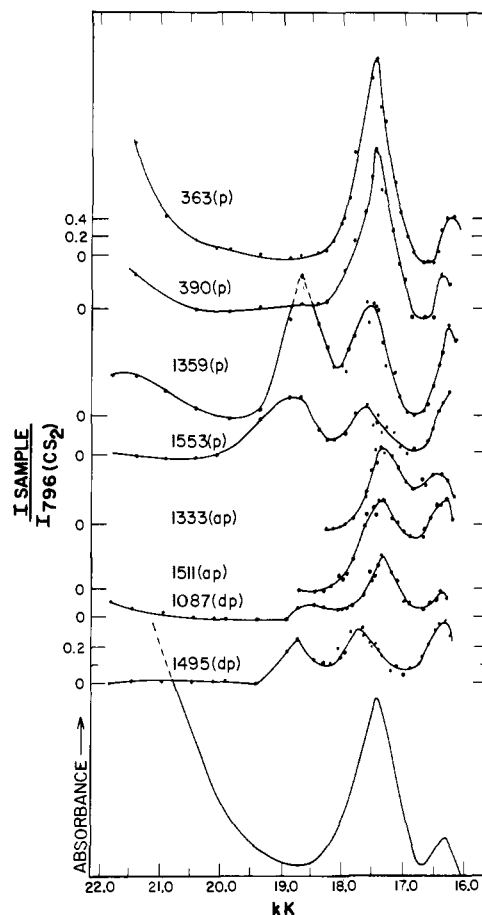
by the relatively large profile bandwidths (~400 cm^{-1}).[23] Shelnutt et al.[1b] suggest that coupling between vibronic levels also contributes to the reduction in peak separation as well as the bandwidth. Such coupling can also be invoked to account for the unusual 0–1/0–0 relative intensities, which are nearly equal for the 1511-cm^{-1} mode, but increase progressively for the lower frequency modes.[24]

The 1087-cm^{-1} depolarized mode excitation profile shows a relative 0–1/0–0 intensity ratio of about 2, as expected for vibronic coupling with nonadiabatic effects included.[1b] The 1495-cm^{-1} (dp) mode shows quite different behavior, however, with 0–0, 0–1, and 0–2 maxima, the scattering amplitudes decreasing smoothly. (It is also the only depolarized mode to appear at wavelengths toward the B band, although its relative intensity is flat in this region.) This behavior is suggestive of Jahn–Teller activity, with significant displacement of the Q state potential minimum along this particular Jahn–Teller active (B$_{1g}$ or B$_{2g}$) normal coordinate.[25]

Several of the polarized modes are only seen at wavelengths approaching the B band. However, the 1359- and 1553-cm^{-1} (p) modes show substantial enhancement in the Q band region, with 0–0, 0–1, and 0–2 maxima. (Unfortunately, the nearby 1561-cm^{-1} (dp) band precludes good intensity measurements for the 1553-cm^{-1} band, but significant 0–2 intensity is definitely seen.) The 390- and 363-cm^{-1} modes are likewise resonant with the Q transition and maximize at the 0–0 position. This maximum may also involve the 0–1 transitions, which would not be resolved. Both modes exhibit second maxima at the 0–1 position of the 1359-cm^{-1} band. This behavior was also seen by Shelnutt et al.[1b] for the 400-cm^{-1} mode of CrTPPCl and characterized as a "helping mode" phenomenon. The

1359-cm^{-1} mode helps the 390- and 363-cm^{-1} modes by virtue of its large origin shift in the Q state (as is evidenced by its own 0–2 scattering peak) which produces nonnegligible values for Franck–Condon products involving scattering into 390- and 363-cm^{-1} final states via an intermediate state with one quantum of excitation in the 1359-cm^{-1} mode. Either A term or B term scattering can be augmented in this way, and the theory has been worked out in detail by Warshel and Dauber.[1c] Helping mode behavior has been observed for azulene,[26] and also for transferrin,[27] although for transferrin a substantial change in excited state vibrational frequency and normal mode composition (Duschinsky effect)[28] may be the dominant effect.

The extent of augmentation of the 363-cm^{-1} mode is quite remarkable. Its intensity at the 1359-cm^{-1} 0–1 position is five times that at the 0–0 position. This mode is the Fe–O–Fe symmetric stretch (see above) and its intensity might be expected to arise from resonance with an $O^{2-} \rightarrow Fe^{3+}$ charge transfer transition which could arguably be coincident with the 1359-cm^{-1} 0–1 position (565 nm). However, this seems too low an energy for charge transfer from oxide to high-spin iron(III). In the analogous μ-oxo dimer of ferric EDTA, no intense absorption is encountered at wavelengths longer than 350 nm.[29] Consequently, we are forced to conclude that the 1359-cm^{-1} mode very strongly "helps" the 363-cm^{-1} mode. It is at first glance surprising that the low-frequency bridge mode should be coupled at all to a high-frequency in-plane porphyrin mode. The 1359-cm^{-1} mode undoubtedly has a similar eigenvector to that of the ~1365-cm^{-1} mode of pyrrole-substituted porphyrins, which ^{15}N substitution has shown to involve the largest pyrrole nitrogen motion among the totally symmetric porphyrin modes.[18] Motion of the nitrogen and iron atoms can be expected to be correlated. In Fe(TPP)$_2$O the Fe–N bond distance, 2.087 Å,[19a] which is characteristic for high-spin iron(III), is ~0.08 Å longer than the unconstrained radius of the circle of pyrrole nitrogen atoms.[17] Motion of the iron atom into the circle is made easier if the nitrogen atoms simultaneously move outward. This provides a mechanism for coupling the 363-cm^{-1} Fe–O–Fe stretch with the 1359-cm^{-1} nitrogen breathing mode.

D. Phenyl Ring Interaction. The appearance of Raman bands assignable to internal modes of the phenyl rings, in resonance with the porphyrin π–π* transition, demonstrates an interaction between the phenyl and porphyrin π systems. This interaction does not necessarily refer to the ground state, however, as has been implied.[16a] The phenyl rings are known to be tilted with respect to the porphyrin ring, by angles from 21 to 90°, and there is a substantial barrier to rotation,[30] reflecting the steric hindrance between the ortho hydrogen atoms of the phenyl groups and the adjacent pyrrole rings. π overlap in the ground state is therefore expected to be slight. Consistent with this is the deduction from NMR data[31] that in high-spin ferric TPPs the contact shifts of the phenyl protons are attenuated by more than a factor of 10 in comparison with the meso H shift in porphyrins with methine hydrogen atoms. Moreover, the available structure data indicate no significant differences in porphyrin geometry between TPPs and corresponding derivatives of porphyrins without phenyl groups. Resonance enhancement of Raman intensities depends on Franck–Condon or vibronic factors in the resonant excited state. Consequently, phenyl interaction in the excited state is sufficient to account for resonance enhancement of phenyl modes.

It is possible that excited-state phenyl interaction also accounts for another marked difference between TPP and non-phenyl porphyrin RR spectra. For the latter, non-totally symmetric modes are dominant in the Q band region, while for TPPs, totally symmetric modes are dominant. Evidently, the origin shifts for some totally symmetric modes are larger for

porphyrins with meso phenyl substituents than for those without phenyl groups. This is also apparent from the 0–2 maxima observed in CrTPPCl[16] and [Fe(TPP)]$_2$O. These larger origin shifts may be related to the same steric hindrance that forces the phenyl groups to rotate out of the porphyrin plane in the ground state. The porphyrin Q transition transfers electron density to the meso carbon atoms and provides a driving force for rotation of the phenyl groups into the porphyrin plane, allowing for electron delocalization via the phenyl π system. The energy of the excited state can be lowered by movement of the porphyrin along normal coordinates which relieve the steric hindrance to phenyl rotation.

The modes with 0–2 maxima are associated with bonds that are internal to the pyrrole rings: 1359 cm^{-1} (A_{1g}), assigned to $\nu(C_\alpha$–N); 1495 cm^{-1} (B_{1g}), assigned to $\nu(C_\beta$–C_β); and 1553 cm^{-1} (A_{1g}), also assigned to $\nu(C_\beta$–C_β). The large origin shifts indicated for these modes might arise from ruffling of the pyrrole rings (S_4 distortion[17]) which would allow simultaneous phenyl rotation into the plane. The resultant loss in porphyrin conjugation would change the bond orders internal to the pyrrole rings, and produce large origin shifts for these bond stretching modes. A difficulty with this argument is that $\nu(C_\alpha$–$C_m)$ and $\nu(C_m$–Ph) modes might also be expected to display large origin shifts, since the C_α–C_m and C_m–Ph bond orders would also be altered in the excited state. No significant Q band enhancement is seen for the bands assigned to these modes. However, it is possible that the expected origin shifts are effectively quenched by the kinematic coupling between these modes (discussed in the section on band assignments above).

In summary, the appearance of resonance-enhanced phenyl modes and the strong Q-band activity shown by totally symmetric porphyrin modes, and at least one Jahn–Teller mode, might all be understood qualitatively if excitation is accompanied by a rotation of the phenyl groups into the porphyrin plane, resulting in charge delocalization and a large origin shift for those modes that relieve the steric hindrance.

References and Notes

(1) (a) J. A. Shelnutt, D. C. O'Shea, N. T. Yu, L. D. Cheung, and R. H. Felton, *J. Chem. Phys.*, **64**, 1156 (1976); (b) J. A. Shelnutt, L. D. Cheung, R. C. C. Chang, N. T. Yu, and R. H. Felton, *ibid.*, **66**, 3387 (1977); (c) A. Warshel and P. Dauber, *ibid.*, **66**, 5477 (1977); (d) S. Asher and K. Sauer, *ibid.*, **64**, 4115 (1976).
(2) (a) T. G. Spiro and J. M. Burke, *J. Am. Chem. Soc.*, **98**, 5482 (1976); (b) L. D. Spaulding, C. C. Chang, N. T. Yu, and R. H. Felton, *ibid.*, **97**, 2517 (1975); (c) A. Warshel, *Annu. Rev. Biophys. Bioeng.*, **6**, 273 (1977).
(3) (a) R. R. Gaughan, D. F. Shriver, and L. J. Boucher, *Proc. Natl. Acad. Sci. U.S.A.*, **72**, 433 (1975); (b) F. Adar and T. S. Srivastava, *ibid.*, **72**, 4419 (1975); (c) R. Mendelsohn, S. Sunder, and H. J. Bernstein, *J. Raman Spectrosc.*, **3**, 303 (1975).
(4) (a) D. H. O'Keeffe, C. H. Barlow, G. A. Smythe, W. H. Fuchsman, T. H. Moss, H. R. Lilienthal, and W. S. Caughey, *Bioinorg. Chem.*, **5**, 125 (1975); (b) G. N. LaMar, G. R. Eaton, R. H. Holm, and F. A. Walker, *J. Am. Chem. Soc.*, **95**, 63 (1973).
(5) (a) J. S. Leigh, D. F. Wilson, C. S. Oren, and T. E. King, *Arch. Biochem. Biophys.*, **160**, 476 (1974); (b) B. F. Van Gelder and H. Beinert, *Biochim. Biophys. Acta*, **189**, 1 (1969); (c) B. G. Malmstrom, *Q. Rev. Biophys.*, **6**, 389 (1973).
(6) L. L. Shipman, T. M. Cotton, J. R. Norris, and J. J. Katz, *Proc. Natl. Acad. Sci. U.S.A.*, **73**, 1791 (1976); F. K. Fong, *ibid.*, **71**, 3692 (1974).
(7) G. H. Barnett, M. F. Hudson, and K. M. Smith, *Tetrahedron Lett.*, **30**, 2887 (1973).
(8) (a) J. Fajer, D. C. Borg, A. Forman, R. H. Felton, L. Vegh, and D. Dolphin, *Ann. N.Y. Acad. Sci.*, **206**, 349 (1973); (b) A. D. Adler, F. R. Longo, J. D. Finarelli, J. Goldmacher, J. Assour, and L. Korsakoff, *J. Org. Chem.*, **32**, 476 (1967); (c) A. D. Adler, F. R. Longo, F. Kampas, and J. Kim, *J. Inorg. Nucl. Chem.*, **32**, 2443 (1970).
(9) T. G. Spiro and T. C. Strekas, *J. Am. Chem. Soc.*, **96**, 338 (1974).
(10) T. G. Spiro and T. C. Strekas, *Proc. Natl. Acad. Sci. U.S.A.*, **69**, 2622 (1972).
(11) J. R. Nestor and T. G. Spiro, *J. Raman Spectrosc.*, **1**, 539 (1973).
(12) T. Kitagawa, H. Ogoshi, E. Watanabe, and Z. Yoshida, *J. Phys. Chem.*, **79**,

2629 (1975).

(13) T. R. Nanney, R. J. Bailey, and E. R. Lippincott, *Spectrochim. Acta*, **21**, 1495 (1965).

(14) R. J. Jokobsen, *Spectrochim. Acta*, **21**, 127 (1965).

(15) A. Bree, C. Y. Pang, and L. Rabeneck, *Spectrochim. Acta, Part A*, **27**, 1293 (1971).

(16) (a) W. H. Fuchsman, Q. R. Smith, and M. M. Stein, *J. Am. Chem. Soc.*, **99**, 4190 (1977); (b) W. H. Fuchsman, private communication.

(17) J. L. Hoard, "Porphyrins and Metalloporphyrins", K. M. Smith, Ed., American Elsevier, New York, N.Y., 1975, p 317.

(18) (a) T. Kitagawa, M. Abe, Y. Kyogoku, H. Ogoshi, H. Sugimoto, and Z. Yoshido, *Chem. Phys. Lett.*, **48**, 55–58 (1977); (b) J. Kincaid, P. Stein, D. Shemin, and T. G. Spiro, to be published.

(19) (a) A. B. Hoffman, D. M. Collins, V. W. Day, E. B. Fleischer, T. S. Srivastava, and J. L. Hoard, *J. Am. Chem. Soc.*, **94**, 3618 (1972); (b) E. Fleischer and T. S. Srivastava, *ibid.*, **91**, 2403 (1969).

(20) R. M. Wing and K. P. Callahan. *Inorg. Chem.*, **8**, 871 (1969).

(21) T. C. Strekas, D. H. Adams, A. Packer, and T. G. Spiro, *Appl. Spectrosc.*, **28**, 324 (1974).

(22) J. Friedman and R. M. Hochstrasser, *Chem. Phys. Lett.*, **32**, 414 (1975); M. Zerner and M. Gouterman, *Theor. Chim. Acta*, **6**, 363 (1966).

(23) G. Barth, R. E. Linder, E. Bunnenberg, and C. Djerassi, *Ann. N.Y. Acad. Sci.*, **206**, 223 (1973).

(24) S. Hassing and O. S. Mortensen, *Chem. Phys. Lett.*, **47**, 115 (1977).

(25) M. Tsuboi and A. Y. Hirakawa, *J. Mol. Spectrosc.*, **56**, 146 (1975).

(26) R. Liang, O. Schnepp, and A. Warshel, *Chem. Phys. Lett.*, **44**, 394 (1976).

(27) B. P. Gaber, V. Miskowski, and T. G. Spiro, *J. Am. Chem. Soc.*, **96**, 6868 (1974).

(28) F. Duschinsky, *Acta Physicochim. URSS*, **1**, 551 (1973).

(29) H. B. Gray, *Adv. Chem. Ser.*, **No. 100**, 365 (1971).

(30) S. S. Eaton and G. R. Eaton, *J. Am. Chem. Soc.*, **97**, 3660 (1975).

(31) G. N. LaMar, G. R. Eaton, R. H. Holm, and F. A. Walker, *J. Am. Chem. Soc.*, **95**, 63 (1973).

Structure-Sensitive Resonance Raman Bands of Tetraphenyl and "Picket Fence" Porphyrin–Iron Complexes, Including an Oxyhemoglobin Analogue

J. M. Burke,[1a] **J. R. Kincaid,**[1a] **S. Peters,**[1b] **R. R. Gagne,**[1b] **J. P. Collman,**[1b] **and T. G. Spiro***[1a]

Contribution from the Department of Chemistry, Princeton University, Princeton, New Jersey 08540, and the Department of Chemistry, Stanford University, Stanford, California 94305. Received March 13, 1978

Abstract: Resonance Raman spectra are reported for iron *meso*-tetraphenylporphine (TPP) and *meso*-tetra($\alpha,\alpha,\alpha,\alpha$-*o*-pivaloylamidophenyl)porphine ($T_{piv}PP$), in 2+ and 3+ oxidation states and in high, low, and intermediate (Fe^{2+}) spin states. Non-totally symmetric modes are seen weakly, or are absent, and only polarized modes can be monitored through the series of complexes. Three of these, ~390, ~1360, and ~1560 cm^{-1}, show appreciable frequency shifts associated with oxidation and spin-state changes. The vibrational signature of the five-coordinate (high-spin) Fe^{2+} complexes is particularly distinct. The $Fe-O_2$ stretching mode of $Fe(T_{piv}PP)(1\text{-MeIm})O_2$ is located at 568 cm^{-1} (confirmed utilizing $^{18}O_2$), very close to its value in oxyhemoglobin (567 cm^{-1}). This relatively high frequency is consistent with appreciable multiple bond character for the $Fe-O_2$ bond.

Introduction

In systematic studies of metalloporphyrin chemistry, *meso*-tetraphenylporphine (TPP) is frequently the molecule of choice because of its convenient synthesis. Although the pattern of peripheral substitution (see Figure 1, ref 6a) is very different from that of physiological porphyrins, extensive comparison of crystal structure determinations suggests that the bonding within the porphinato core is essentially the same in both porphyrin classes.[2a] Recently, the TPP framework has been used to erect a "picket fence", in the form of pivaloylamide groups substituted at the *o*-phenyl positions, with the aim of providing a protected coordination environment.[2b] This approach led to the preparation of the first (and so far only) isolable, crystalline dioxygen complex of an iron porphyrin.[3] Its crystal structure reveals the Fe–O–O unit to be bent, as in the Pauling model for oxyhemoglobin.

Resonance Raman (RR) spectroscopy has been extensively applied to heme proteins[4] and metalloporphyrin[5] analogues. Vibrational modes of the porphyrin ring can be monitored with high sensitivity, and are observed to shift frequency in a characteristic manner[4] which is associated with the oxidation state or axial ligation of the central metal atom. Protein influence on porphyrin structure can be evaluated from the vibrational pattern. Tetraphenylporphyrins give RR spectra that are quite different in appearance from those of physiological porphyrins, and while numerous TPP spectra have been reported,[6] no structural interpretations have been offered.

We have examined the vibrational patterns of a series of iron TPP complexes, several of whose crystal structures are available, and of a corresponding series of $T_{piv}PP$ [*meso*-tetra($\alpha,\alpha,\alpha,\alpha$-*o*-pivaloylamidophenyl)porphine] complexes. While the structural utility of the data is more limited than for the physiological porphyrins, three structure-sensitive bands are identified. The vibrational pattern for five-coordinate (high-spin) iron(II) derivatives is particularly distinct. The iron–oxygen stretching mode of the "picket fence" dioxygen complex has been identified at 568 cm^{-1}. Its frequency is close to that observed for oxyhemoglobin (567 cm^{-1})[7] and establishes the similarity of the iron–oxygen bond in protein and analogue. The relatively high frequency is consistent with substantial multiple bond character.

Experimental Section

meso-Tetraphenylporphine was purchased from Aldrich Chemical Co., Inc. Treatment with 2,3-dichloro-5,6-dicyanobenzoquinone and chromatography on alumina (Fisher A-540) removed all traces of tetraphenylchlorin.[8] The iron(III) complexes and β carbon deuterated species were prepared as indicated previously.[6a] The synthesis of *meso*-tetra($\alpha,\alpha,\alpha,\alpha$-*o*-pivaloylamidophenyl)porphineiron(III) bromide has been described.[2] The iron(II) complexes were prepared in situ by reduction of a methylene chloride solution of the iron(III) complex with aqueous sodium dithionite.[5a]

The bisimidazole (1m), 1-methylimidazole (1-MeIm), and 2-methylimidazole (2-MeIm) iron(II) (TPP) and $T_{piv}PP$ derivatives gave resonance Raman spectra which indicated the presence of ad-